

Molecular Dynamics Simulations to Investigate the Effects of Zinc Ions on the Structural Stability of the c-Cbl RING Domain

Hsuan-Liang Liu,^{*,†,‡} Ching-Tao Yang,[†] Jian-Hua Zhao,[†] Chih-Hung Huang,[‡] Hsin-Yi Lin,[‡] Hsu-Wei Fang,[†] Yih Ho,[§] and Wei-Bor Tsai^{||}

Department of Chemical Engineering and Biotechnology and Graduate Institute of Biotechnology, National Taipei University of Technology, 1 Section 3 ZhongXiao East Road, Taipei, Taiwan 10608, School of Pharmacy, Taipei Medical University, 250 Wu-Hsing Street, Taipei, Taiwan 110, and Department of Chemical Engineering, National Taiwan University, 1 Section 4 Roosevelt Road, Taipei, Taiwan 106

In eukaryotic cells, ubiquitylation of proteins plays a critical role in regulating diverse cell processes by the ubiquitin activating enzyme (E1), ubiquitin-conjugating enzyme (E2), and ubiquitin protein ligase (E3). E3 is the key component that confers specificity to ubiquitylation and directs the conjugation of ubiquitin to a specific target protein. RING domains are small structured protein domains that require the coordination of zinc ions for a stable tertiary fold and some of them are involved in the E3 family. In this study, we reported the detailed relationships between the two zinc ions and the structural stability of the c-Cbl RING domain by molecular dynamics simulations. Our results show that these two zinc ions play an important role in maintaining both the secondary and tertiary structural stabilities of the c-Cbl RING domain. Our results also reveal that the secondary structural stability of the c-Cbl RING domain is mainly determined by the hydrogen-bonding networks in or near the two zinc ion binding sites. Our results further demonstrate that zinc ion binding site 2 is more structurally stable than site 1.

Introduction

The process of ubiquitylation involves multiple steps and requires at least three proteins: the ubiquitin activating enzyme (E1), ubiquitin-conjugating enzyme (E2), and ubiquitin protein ligase (E3) (1–3). Two major families of E3 have been identified: HECT proteins and RING domain containing proteins. Although not all proteins that contain a RING domain belong to E3, a large and growing number of RING proteins have been found to exhibit ubiquitin–ligase activity.

It has been shown that Cbl family exhibits E3 ubiquitin–ligase activity (4–6). This activity is mediated by its RING domain, which is essential to recruit a specific E2 into the active signaling complexes (5–7). The overall structure of Cbl family can be divided into several recognizable domains as follows: (i) a phosphotyrosine recognition domain; (ii) a zinc-coordinating Cys3-His-Cys4 (C3HC4) RING finger ubiquitin–ligase domain; (iii) a proline-rich region; and (iv) a leucine zipper motif. Each of these domains has been shown to interact with signaling proteins upon activation (8–11).

The c-Cbl protein is one of the members in the Cbl family. A recent crystal structure of c-Cbl complexed with the human ubiquitin-conjugating enzyme 7 (UbcH7) has provided detailed information regarding the structure and function of the c-Cbl RING domain (12). The RING domain, containing a C3HC4 motif, is located at the C-terminus of c-Cbl from amino acid

residues 380 to 434 (Figure 1 A). The overall structure is similar to the crystal structure of the RAG1 RING domain (13). The c-Cbl RING domain consists of a shallow groove consisting of the helix and the two zinc-chelating loops (14). This groove, composed of six residues, not only accommodates the most significant contacts toward UbcH7 recognition, but also serves as a structural feature that applies the c-Cbl RING domain to function as an ubiquitin ligase (12).

One of the distinguished features of the c-Cbl RING domain is the presence of a zinc-binding motif containing two tetrahedrally coordinated zinc ions that stabilizes its globular structure (Figure 1B) (12). Four pairs of metal-binding residues sequester two zinc ions at distinct tetrahedral sites forming a “cross-brace” motif (Figure 1C) (15). In this motif, the first and third pairs bind one zinc ion, while the second and fourth pairs bind the other. The other common feature of all C3HC4 structures is the 14 Å distance between the two coordinated zinc ions and the presence and length of the secondary structural elements in the RING domain (16).

The stability of the RING domain is a vital requirement for c-Cbl proteins to function as E3 ligases. In this study, detailed relationships between the two zinc ions and the structural stability of the c-Cbl RING domain were reported. To understand which zinc ion is more important in maintaining the structural stability of the c-Cbl RING domain, several molecular dynamics (MD) simulations were conducted toward this domain associated with four zinc-ion binding states: (+, +), (+, –), (–, +), and (–, –), where the former and the later positions in the bracket represent the first and the second zinc ion binding sites, denoted as S1 and S2, respectively, and + and – indicate having and not having zinc ion in the corresponding zinc ion binding site, respectively. For example, the binding state

* Corresponding author. E-mail: f10894@ntut.edu.tw. Phone: +886-2-27712171, ext. 2542. Fax: +886-2-27317117.

[†] Department of Chemical Engineering and Biotechnology, National Taipei University of Technology.

[‡] Graduate Institute of Biotechnology, National Taipei University of Technology.

[§] Taipei Medical University.

^{||} National Taiwan University.

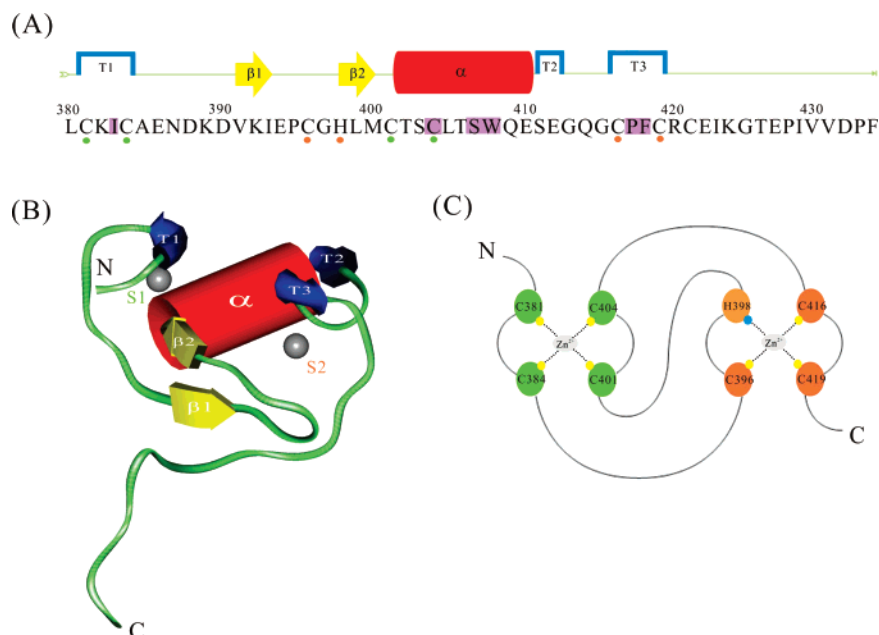


Figure 1. (A) Amino acid sequence of the c-Cbl RING domain with the locations of the secondary structural elements indicated on the top of the sequence. The six residues forming the contact “groove” involved in UbcH7 recognition are highlighted in purple. The residues involved in the binding of zinc ion in S1 and S2 are marked with green and orange dots, respectively. (B) The 3D structure of the c-Cbl RING domain, which is extracted from the crystal structure of the c-Cbl-UbcH7 complex (12). The locations of S1, S2, α , β , and turn are indicated. The N- and C-termini are labeled as N and C, respectively. The two zinc ions are shown as gray spheres. (C) Schematic representation of the ligation scheme employed by the c-Cbl RING domain showing the unique “cross-brace” motif (15). Green and orange ellipses represent the residues forming S1 and S2, respectively. The two zinc ions are shown in gray ellipses. Sulfur and nitrogen atoms involved in directly chelating with zinc ions are shown as yellow and blue spheres, respectively. The N- and C-termini are labeled as N and C, respectively.

(+, +) indicates the c-Cbl RING domain having both S1 and S2 binding with zinc ions.

Methods

The Construction of the c-Cbl RING Domain Structures Associated with Four Zinc Ion Binding States. The X-ray crystallographic structure of the c-Cbl-UbcH7 complex was obtained from the Protein Data Bank (PDB: 1FBV) (12). The c-Cbl RING domain was isolated from chain A with amino acid residues from 380 to 434 (Figure 1A) and the resulting structure after minimization is shown in Figure 1B. The c-Cbl RING domain associated with four zinc ion binding states, denoted as (+, +), (+, -), (-, +), and (-, -), were generated by the method described previously (17).

Molecular Dynamics Simulations. The molecular minimization and dynamics simulations were carried out using Discover 2.9.8 in the SGI Tezro workstation (Silicon Graphics, Mountain View, CA) and a Linux-PC platform with the consistent valence force field (CVFF) (18). All the calculations were performed using NVT and periodic boundary conditions (PBC) with the cutoff radius being 12 Å for both nonbonded electrostatic and van der Waals interactions. The four types of the c-Cbl RING domain were submitted to 5000 iterations with steepest gradient method, followed by 5000 iterations with conjugated gradient method. Each energy-minimized c-Cbl RING domain was placed in the center of a pseudo-unit cell with the size of $50 \times 60 \times 40 \text{ \AA}^3$ soaked with water molecules. First, solvent alone was minimized for 5000 steps, followed by the minimization of the protein alone with 5000 steps. Then, the entire system was energy-minimized until the maximum derivative was lower than $0.001 \text{ kcal mol}^{-1} \text{ \AA}^{-1}$. Finally, several 2 ns MD simulations with 100 ps in equilibrium were carried out for these systems with constant temperature constraint at 298 and 498 K. The time step of the MD simulations was set as 1 fs.

Structural Analysis. The trajectories saved every 10 ps were analyzed using Analysis module of the InsightII program (Accelrys, San Diego, CA). The C_α root mean square deviation (RMSD), solvent accessible surface area (SASA), and the averaged distance (D) between the mass centers of the four zinc ion binding atoms in S1 and S2 were calculated. Secondary structural analysis was carried out according to DSSP (19). The detailed relationship between the secondary structure content and the stability of the zinc ion binding sites was determined using the analysis of the numbers of the native hydrogen bonds. The native hydrogen-bond persistence maps were constructed by calculating the fraction of the native hydrogen bonds in the defined locations during the entire MD simulations. These defined locations are listed as follows: (S1) zinc ion binding site 1; (S1- α) the region between S1 and α ; (α) secondary structure element α -helix; (S2) zinc ion binding site 2; (S2-T3) the region between S2 and T3; (T3) secondary structure turn 3. The hydrogen bonds in the defined locations together form the hydrogen-bonding networks in or near the two zinc ion binding sites. The detailed information of these native hydrogen bonds is summarized in Table 1.

Results and Discussion

The Effects of the Two Zinc Ions on the Tertiary Structural Stability of the c-Cbl RING Domain. In this study, several MD simulations were performed to investigate the structural fluctuations of the c-Cbl RING domain associated with four zinc ion binding states to investigate the effects of the two zinc ions on the structural stability of this domain. Usually, the analyses of RMSD and SASA are used as a powerful strategy in determining the tertiary structural fluctuations of the target protein. The RMSD and SASA data for the c-Cbl RING domain associated with four zinc ion binding states during the entire MD simulation courses at 298 and 498 K are

Table 1. Detailed Information of the Native Hydrogen Bonds in Various Locations of the c-Cb1 Ring Domain

location	donor	acceptor	type ^a
S1	C401/HN	C381/S γ	M-S
	C404/HN	C401/O	M-M
	C404/HN	C401/S γ	M-S
S1- α	C404/HN	C401/O	M-M
	C404/HN	C401/S γ	M-S
	L405/HN	C401/O	M-M
α	W408/HN	C404/O	M-M
	S403/H γ	S403/O	M-S
	T406/HN	T402/O	M-M
	T406/HG	T406/O	M-S
	S407/HN	S403/O	M-M
	W408/HN	L405/O	M-M
	Q409/HN	L405/O	M-M
	E410/HN	T406/O	M-M
S2	H398/N δ 1	C396/S γ	S-S
	H398/N δ 1	C416/S γ	S-S
	H398/N δ 1	C419/S γ	S-S
S2-T3	C419/HN	C416/S γ	M-S
	P417/N	C416/S γ	M-S
T3	F418/HN	C416/S γ	M-S
	P417/N	C416/S γ	M-S
	F418/HN	C416/S γ	M-S
	C419/HN	C416/S γ	M-S

^a M-M, main chain-main chain; M-S, main chain-side chain; S-S, side chain-side chain.

shown in Figure 2 A and B, respectively. At 298 K, the RMSD and SASA values for the c-Cb1 RING domain associated with the four zinc ion binding states are very similar, indicating that, at low simulation temperature, the entire tertiary structure of the c-Cb1 RING domain remains relatively stable with or without zinc ion binding in S1 and S2. However, it is obvious that elevated simulation temperature provides higher kinetic energy to facilitate the structural fluctuations, where the c-Cb1 RING domain with and without both zinc ions binding in S1 and S2 exhibit the most and the least structural stability, respectively. The relationship between the averaged RMSD and the averaged SASA for the c-Cb1 RING domain associated with four zinc ion binding states at 498 K is shown in Figure 2C. A positive correlation between these two properties for this domain was observed at elevated simulation temperature. The result shows that both RMSD and SASA of the c-Cb1 RING domain increase when either one or both zinc ions are removed from S1 and S2. It further indicates that the c-Cb1 RING domain acquires its structural stability through the binding of both zinc ions to S1 and S2. Our results also demonstrate that S2 seems to play a slightly more important role than S1 in maintaining the tertiary structural stability of this domain, as can be seen from the trajectories of RMSD and SASA in Figure 2 panels A and B, respectively, and the linear relationship presented in Figure 2C.

The averaged RMSD values of S1, S2, and the six residues forming the "groove" involved in UbCh7 recognition for the c-Cb1 RING domain associated with four zinc ion binding states at 298 and 498 K are plotted in Figure 3 panels A and B, respectively. At low simulation temperature, these averaged RMSD values are mostly less than 2 Å, indicating that these local structural elements remain stable with or without either one or two zinc ions binding to S1 and S2. However, it is obvious that S1 and S2 exhibit more structural fluctuations compared to each other when the first and the second zinc ions are removed from their corresponding zinc ion binding sites. It suggests that the binding of the two zinc ions indeed stabilizes both S1 and S2. The results at elevated temperature also show the similar trend. Interestingly, the removal of either one or two zinc ions seems to influence the UbCh7 recognition site more

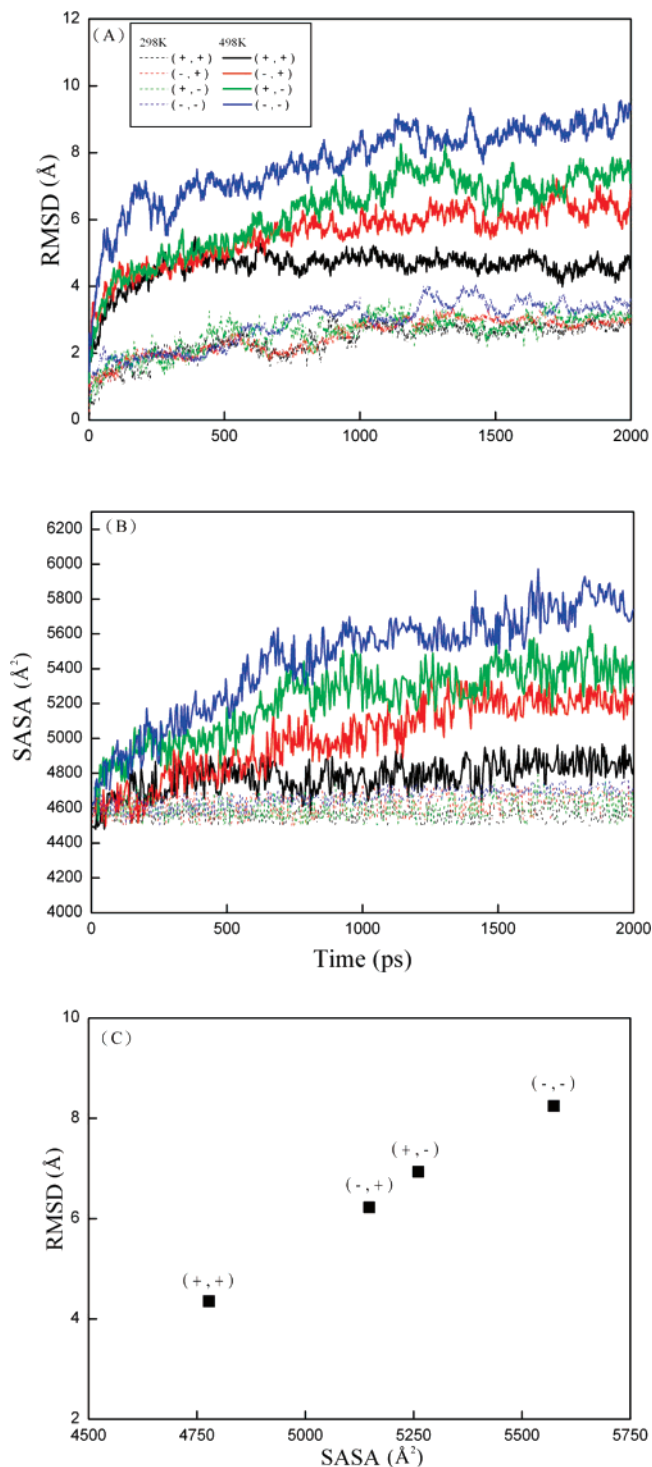


Figure 2. (A) Backbone RMSD and (B) SASA of the c-Cb1 RING domain associated with four zinc ion binding states at 298 and 498 K during the MD simulation courses; (C) the relationship between the averaged rmsd and the averaged SASA for the c-Cb1 RING domain associated with four zinc ion binding states at 498 K.

significantly than S1 and S2. It indicates that these two zinc ions not only play a crucial role in maintaining the structural stability of the c-Cb1 RING domain, but also play an important role in regulating UbCh7 recognition, which is in good agreement with the previous study showing that the zinc finger motif is involved in protein-protein interactions (16). The above analyses all indicate that these two tetrahedrally coordinated zinc ions not only play an important role in maintaining the important local structural stability of S1, S2, and UbCh7

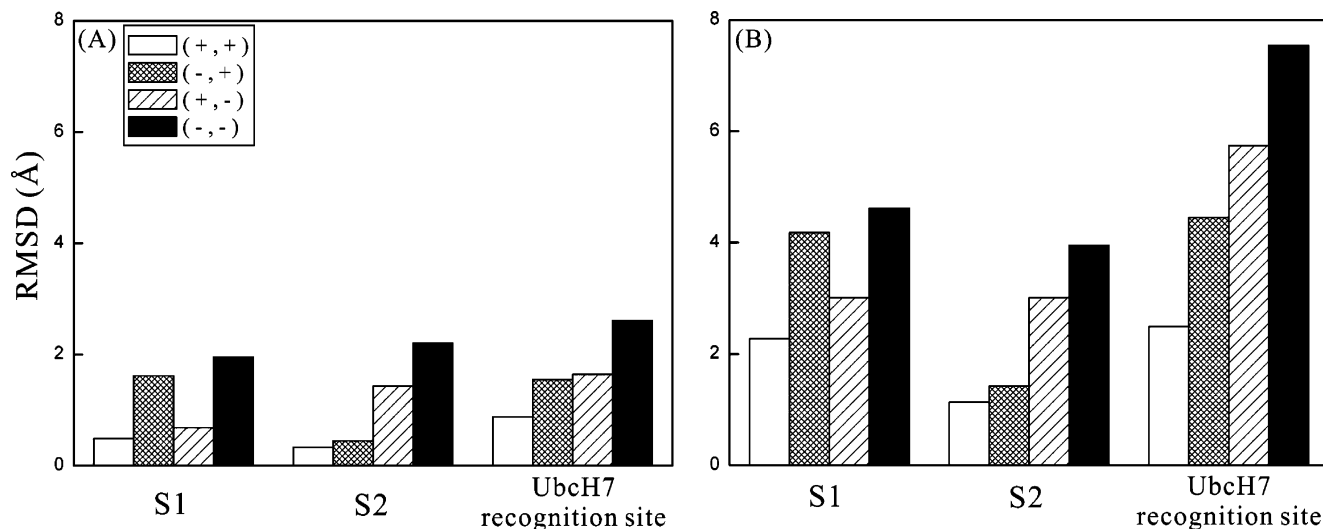


Figure 3. Averaged backbone RMSD of S1, S2, and the six residues forming the contact “groove” involved in Ubch7 recognition at (A) 298 and (B) 498 K.

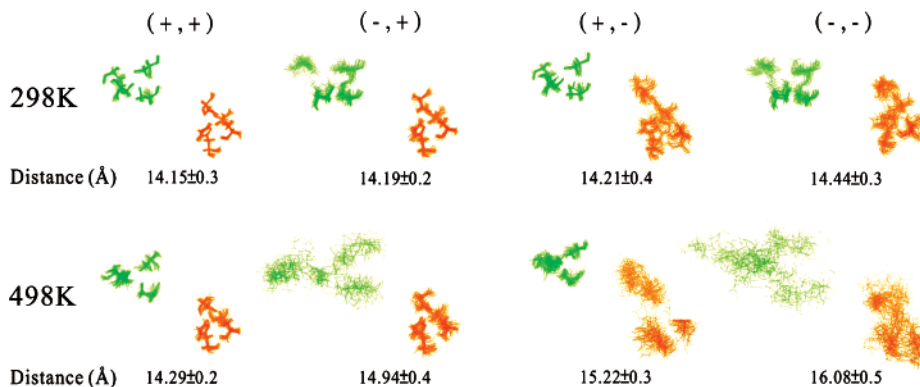


Figure 4. Superimpositions of the heavy atoms of S1 and S2 obtained from the snapshots during the MD simulations at both 298 and 498 K. The residues involved in S1 and S2 are colored green and orange, respectively. The averaged distances between the mass centers of the four zinc ion chelated atoms in S1 and S2 are listed under their corresponding structures.

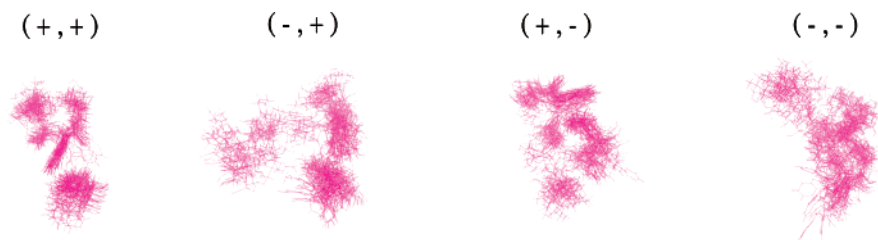


Figure 5. Superimpositions of the heavy atoms of the six residues forming the contact “groove” involved in Ubch7 recognition obtained from the snapshots during the MD simulations at 498 K.

recognition site but also contribute to stabilize the tertiary structure of the entire c-Cbl RING domain.

Although there is no direct interaction between S1 and S2 as observed from their amino acid sequences given in Figure 1A and the “cross-brace” motif (15) shown in Figure 1C, their dynamics properties would be affected by each other. When one zinc ion binding site of the c-Cb1 RING domain is chelated with zinc ion, the structure of the other site would be more compact whether it is chelated with zinc ion or not. In contrast, the structure of one zinc ion binding site would be more flexible when the other site is not chelated with zinc ion. In other words, the structural stability of S1 and S2 is dependent on each other. Previous studies about the thermodynamics properties of zinc ion binding have shown that a “cross-brace” RING domain should bind zinc ions with negative cooperativity (15). That is, when zinc ion is chelated with S1 before S2, the already chelated

S1 may lead to the destabilization of the local structure of the empty S2 (20, 21). The results of the present MD simulations also indicated that these two zinc ion binding sites influence the structural stability of each other with negative cooperativity (see Figure 3).

Despite the positive effects of these two zinc ions on the structural stability of S1, S2, and the entire c-Cb1 RING domain, they also enhance the structural integrity of Ubch7 recognition site, as can be seen in Figure 3. Such high specificity of recognition helps the RING E3s to distinguish a specific E2 from the diverse E2 family during ubiquitinylation. Remarkably, the structural stability of this Ubch7 recognition site is controlled by both zinc ions. This specific feature is originated from the regulation of both S1 and S2 to confer a suitable conformation for these six residues to form a stable contact groove toward Ubch7 recognition. Our results are in good

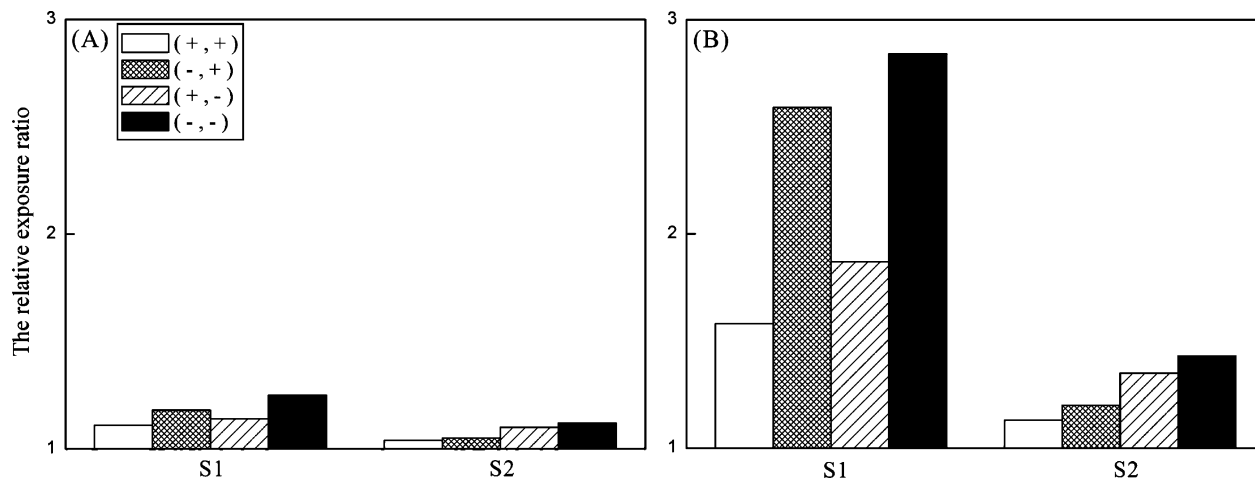


Figure 6. The relative exposure ratios of S1 and S2 of the c-Cb1 RING domain associated with four zinc ion binding states at (A) 298 and (B) 498 K.

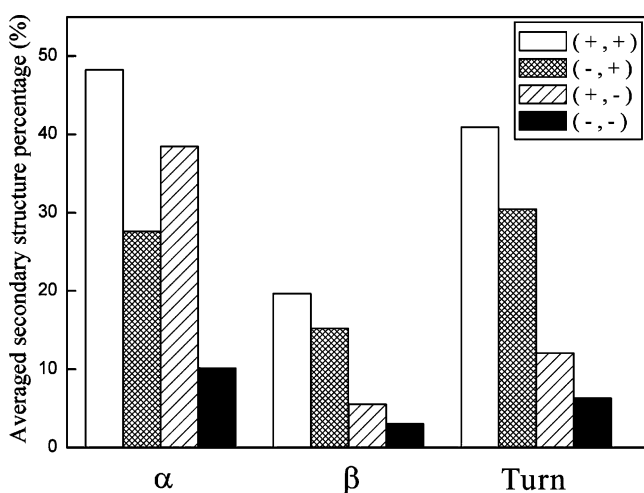


Figure 7. The averaged secondary structures of the c-Cb1 RING domain associated with four zinc ion binding states during the MD simulations at 498 K.

agreement with previous study showing that structural integrity of the RING groove has a central role in determining the specificity of the c-Cb1 E3 for E2 (12), which is supported by several examples of evidence of mutagenesis. The structural integrity of UbcH7 recognition site also provides a framework to help identify the cognate E2s for the large number of RING E3 proteins. Currently, several molecular simulations are conducting for c-Cb1 (C3HC4), CNOT4 (C4C4), and p44 (C4C4) in our group. The former two RING domain exhibits E2 recognition function, whereas the later one does not. Our results show that zinc ion-related structural stability of the RING domain is an important feature for E2 recognition (unpublished data).

The superimpositions of the heavy atoms of S1 and S2 and of the six residues forming the contact groove in UbcH7 recognition obtained from the snapshots during the MD simulations are shown in Figures 4 and 5, respectively. These structures all show that the residues involved in S1, S2, and UbcH7 recognition site form unfolded or highly disordered conformations when either one or two zinc ions are removed from the two zinc ion binding sites of the c-Cb1 RING domain, particularly at elevated simulation temperature. It may further imply that the folding of the c-Cb1 RING domain may depend on the correct binding of these two zinc ions into S1 and S2. The correctly folded structure further allows the c-Cb1 RING domain to recognize a specific E2 from the diverse E2 family

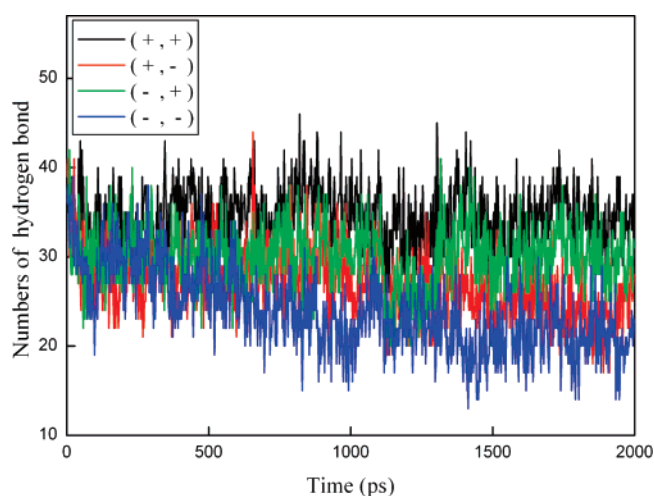


Figure 8. The numbers of hydrogen bonds of the entire c-Cb1 RING domain associated with four zinc ion binding states during the MD simulations at 498 K.

during ubiquitylation. Previous studies also showed that the c-Cb1 RING domain requires high intrinsic stability to provide the necessary stability for the latter complex through protein–protein interaction (16, 22). One of the common features of all C3HC4 structures is the 14 Å distance between the two zinc ions of the zinc-binding motif (16). In Figure 4, we found that this distance (D) ranges from 14.15 Å for the binding state (+, +) to 14.44 Å for the binding state (-, -) at 298 K, indicating that this common structural feature remains well even with the removal of the two zinc ions from S1 and S2 at low simulation temperature. However, D increases from 14.29 for (+, +) to 16.08 Å for (-, -) at 498 K, indicating that elevated simulation temperature could induce structural changes leading to the destruction of this important structural feature of the C3HC4 RING domain, particularly when both two zinc ions are removed from S1 and S2.

Figures 2–5 all provide the information showing that S2 is more important than S1 in maintaining the structural stability of the entire c-Cb1 RING domain and the local structural elements S1, S2, and UbcH7 recognition site. Our results are consistent with the previous study showing that metal binding by and folding around S2 are important for the biological functionality of the RING domain and molecular recognition inherent therein (21). To investigate the detailed structural fluctuations of S1 and S2, the relative exposure ratios, which were calculated by dividing the averaged SASAs of S1 and S2

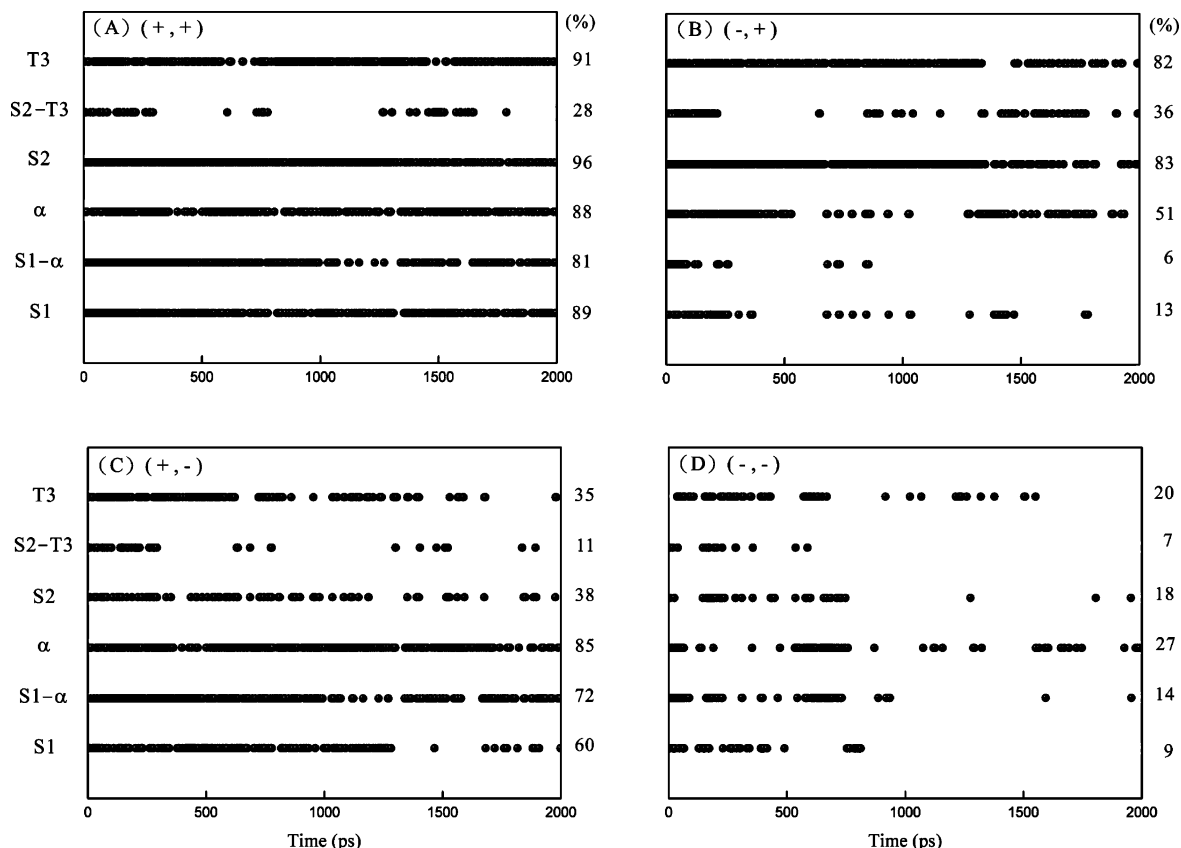


Figure 9. Native hydrogen-bond persistence maps in the defined locations of S1, S1- α , α , S2, S2-T3, and T3 during the MD simulations at 498 K for the c-Cb1 RING domain associated with four zinc ion binding states: (A) (+, +); (B) (-, +); (C) (+, -); and (D) (-, -). The hydrogen-bond fraction higher than 0.5 is presented in black at that time. The averaged native hydrogen-bond persistence percentage for each defined location is listed on its right.

during the MD simulation courses at 298 and 498 K to the SASAs of S1 and S2 in the initial structure, were determined, and the results are presented in Figure 6. The results show that all the relative exposure ratios of S1 and S2 for the c-Cb1 RING domain associated with four zinc ion binding states during the MD simulation course at 298 K are very similar to those of S1 and S2 in the initial structure (Figure 6A). In contrast, all the relative exposure ratios of S1 for the c-Cb1 RING domain associated with four zinc ion binding states are significantly higher than those of S2 at 498 K, comparing to the initial structure. This observation reinforces the fact that S1 exhibits higher structural fluctuation than S2. It may be because S1 is located in the flexible N-terminal region while S2 is more buried in the interior of this domain. However, the present results showing that S2 is more structurally stable than S1 is somewhat in contrast with the previous findings about the C3HC4 RING domain (20, 23). There are two probable explanations: (1) First, an isolated RING domain from the c-Cb1-UbcH7 complex was used as the initial structure in this study. There are many hydrogen bonds and van der Waals contacts among the c-Cb1 TKB domain, the c-Cb1 linker sequence, and the c-Cb1 RING domain in the crystallographic structure of the entire complex (12). These interactions, whose function is to stabilize the structure of the complex, are all located close to the N-terminal region and S1 of the c-Cb1 RING domain. Thus, the vicinity of S1 in the c-Cb1 RING domain is more flexible and exposed to solvent without interacting with the c-Cb1 TKB domain and the c-Cb1 linker sequence. (2) Previous studies all used metal-exchange experiments to determine the stability of the zinc ion binding sites (20, 23). The lower stability of S2 is due to the lower affinity of histidine for zinc ion than of cysteine. This

differential stability is also related to an even lower affinity of the histidine for the cobalt ion. Furthermore, the distinct metal ion exchanging rates are strongly related to the electrostatic surface potential near metal ion binding sites. In addition, the study of the zinc-cadmium exchange by NMR titration experiments using the RING domain of CNOT4 (C4C4) has revealed that the first site exchanges before the second one does (24). As a result, they have indicated that the structure of the C4C4 RING finger of human NOT4 reveals features distinct from those of C3HC4 RING domains. The above experimental results suggest that the lower affinity of the S2 in the RING domain toward metal binding is not a general property for all RING domains and that the affinity of the zinc ion binding site toward various metal ions cannot be directly related to its structural stability.

Previously, Joazeiro et al. (5) examined the effect of several point mutations on c-Cb1 RING Ub ligase activity, and their results showed that Cys381 fits the RING consensus and its mutation to alanine impairs c-Cb1's ability to stimulate ubiquitination of EGF receptor in vivo. Cys381 is one of the four cysteine residues forming S1 (Figure 1), and its replacement with alanine may result in the disruption of the structural integrity of S1, which may further lead to the defection in both ubiquitination and Ubc4 activation assays (5). This well-characterized mutation has been widely used to inactivate c-Cb1 as an E3 ligase. This mutation may also lose its Ub ligase activity through the direct disruption of the contact with E2. It would be of great interest to further investigate the correlation between the structural stability of various important residues of the c-Cb1 RING domain obtained from molecular modeling and their activity obtained from mutagenesis experiments.

The Effects of Zinc Ions on the Secondary Structural Stability of the c-Cbl RING Domain. The averaged secondary structures of the c-Cbl RING domain associated with four zinc ion binding states are shown in Figure 7. It is obvious that the secondary structure contents decrease with removing either one or two zinc ions from S1 and S2, indicating that zinc ions play an important role in maintaining the secondary structural stability of the c-Cbl RING domain. Our results are consistent with the results from the previous study showing that zinc ions induce secondary structure formation in CCHC zinc finger (16). The contents of β and turn are higher for the zinc ion binding state (-, +) than those for (+, -) during the entire MD simulation courses, mainly because of the direct or indirect contacts of S2 with $\beta 1$, $\beta 2$, and T2. In contrast, S1 only influences the structures of T1 and the N-terminal region of α alone (see Figure 2B). It is attributed to the fact that part of S1 is involved in α . Moreover, there are many hydrogen bonds connecting S1 and α either directly or indirectly (see Table 1). Although the contribution of these hydrogen bonds to the structural stability is not as significant as the binding effect of zinc ion in S1, their importance cannot be ignored. Consequently, the α content still remains at a great level during the MD simulation course even when S1 is not binding with zinc ion. In addition to stabilizing α , S1 also plays a role in maintaining the structural stability of T1 at elevated simulation temperature. Unlike β , the content of turn for the zinc ion binding state (-, +) outstrips the content for (-, -) during the simulations. The locations of S1 and T1 are both close to the surface of the c-Cbl RING domain. Thus, the structural stability of S1 may be decreased when it is exposed to the solvent at high simulation temperature. In addition, the flexible N-terminal region also plays a role to disrupt the local secondary structures at elevated simulation temperature. The above results are in good agreement with the previous findings showing that a lower stability of the binding site is observed when it is located near a flexible region (22).

A previous study has observed that the sulfur atoms of the zinc ion binding site which are chelated with zinc ion potentially form N-H...S hydrogen bonds with the closed amide groups ($\leq 3\text{\AA}$) (24). These hydrogen bonds can further contribute to stabilizing the coordination of zinc ions and enhance the stability of the two zinc ion binding sites. Here, we tried to elucidate the molecular relationship between the stability of the zinc ion binding sites and the secondary structure contents by the analysis of the native hydrogen bonds. The numbers of the native hydrogen bonds during the entire simulation courses for the c-Cbl RING domain associated with four zinc ion binding states at 498 K are plotted in Figure 8. Significantly, the number of the native hydrogen bonds of type (+, +) is always higher than that of type (-, -), which is positively correlated to the secondary structure content observed in Figure 7. Figure 9 shows the native hydrogen-bond persistence maps in the defined locations of S1, S1- α , α , S2, S2-T3, and T3 during the MD simulations at 498 K for the c-Cbl RING domain associated with four zinc ion binding states. It shows that α slightly interacts with S1 indirectly and that the number of hydrogen bonds remaining in S2 when it is not chelated with zinc ion is larger than that in S1 when it is not chelated with zinc ion. It again demonstrates that S2 shows higher structural stability than S1 in our MD simulations. In addition, these hydrogen bonds together form a stable hydrogen-bonding network in or near S1 and S2, which contributes significantly in maintaining the secondary structural stability of these two zinc ion binding sites.

Conclusions

So far, many experimental studies have suggested that the high structural stability of the c-Cbl RING domain is attributed to the two zinc ions in the zinc ion binding sites S1 and S2. The structural stability of this domain is necessary for c-Cbl proteins to function as E3 ubiquitin ligases (12). The results of this study showed that both the secondary and tertiary structural stabilities of the c-Cbl RING domain increase with the presence of either one or two zinc ions in S1 and S2. Besides, our results also revealed that the stability of some important structural elements, such as S1, S2, and the UcbH7 recognition site, in the c-Cbl RING domain is mainly determined by the hydrogen-bonding networks in or near the two zinc ion binding sites. Furthermore, we also demonstrated that S2 contributes to the secondary and tertiary structural stability of the c-Cbl RING domain more significantly compared to S1. Our results also supported the previous hypothesis that the folding of the RING domain is in a zinc ion-dependent fashion with the correct coordination of the two zinc ions in S1 and S2 in a tetrahedral format (16). It would be of great interest to compare c-Cbl with other Cbl family members. Currently, several molecular simulations are conducting for c-Cbl (C3HC4), CNOT4 (C4C4), and p44 (C4C4) in our group. The former two-RING domain exhibits E2 recognition function whereas the later one does not. Our results show that zinc ion-related structural stability of the RING domain is an important feature for E2 recognition (unpublished data).

Acknowledgment

The authors gratefully acknowledge the financial support (Project No. NSC 95-2221-E-027-089) from the National Science Council of Taiwan.

References and Notes

- Weissman, A. M. Themes and variations on ubiquitylation. *Mol. Cell Biol.* **2001**, *21*, 169–178.
- VanDemark, A. P.; Hill, C. P. Structural basis of ubiquitylation. *Curr. Opin. Struct. Biol.* **2002**, *12*, 822–830.
- Passmore, L. A.; Barford, D. Getting into position: The catalytic mechanisms of protein ubiquitylation. *Biochem. J.* **2004**, *379*, 513–525.
- Howlett, C. J.; Robbins, S. M. Membrane-anchored Cbl suppresses Hck protein-tyrosine kinase mediated cellular transformation. *Oncogene* **2002**, *21*, 1707–1716.
- Joazeiro, C. A. P.; Wing, S. S.; Huang, H. K.; Levrson, J. D.; Hunter, T.; Liu, Y.-C. The tyrosine kinase negative regulator c-Cbl as a RING-type, E2-dependent ubiquitin-protein ligase. *Science* **1999**, *286*, 309–312.
- Levkowitz, G.; Waterman, H.; Ettenberg, S. A.; Katz, M.; Tsygankov, A. Y.; Alroy, I.; Lavi, S.; Iwai, K.; Reiss, Y.; Ciechanover, A.; Lipkowitz, S.; Yarden, Y. Ubiquitin ligase activity and tyrosine phosphorylation underlie suppression of growth factor signaling by c-Cbl/Sli-1. *Mol. Cell.* **1999**, *4*, 1029–1040.
- Yokouchi, M.; Kondo, T.; Houghton, A.; Bartkiewicz, M.; Horne, W. C.; Zhang, H.; Yoshimura, A.; Baron, R. Ligand-induced ubiquitination of the epidermal growth factor receptor involves the interaction of the c-Cbl RING finger and UbcH7. *J. Biol. Chem.* **1999**, *274*, 31707–31712.
- Thien, C. B. F.; Langdon, W. Y. c-Cbl and Cbl-b ubiquitin ligases: substrate diversity and the negative regulation of signalling responses. *Biochem. J.* **2005**, *391*, 153–166.
- Swaminathan, G.; Tsygankov, A. Y. The Cbl family proteins: ring leaders in regulation of cell signaling. *J. Cell. Physiol.* **2006**, *209*, 21–43.
- Duan, L.; Reddi, A. L.; Ghosh, A.; Dimri, M.; Band, H. The Cbl family and other ubiquitin ligases destructive forces in control of antigen receptor signaling. *Immunity* **2004**, *21*, 7–17.

- (11) Ryan, P. E.; Davies, G. C.; Nau, M. M.; Lipkowitz, S. Regulating the regulator: negative regulation of Cbl ubiquitin ligases. *Trends Biochem. Sci.* **2006**, *31*, 79–88.
- (12) Zheng, N.; Wang, P.; Jeffery, P. D.; Pavletich, N. P. Structure of a c-Cbl-UbcH7 complex: RING domain function in ubiquitin-protein ligases. *Cell* **2000**, *102*, 533–539.
- (13) Bellon, S. F.; Rodgers, K. K.; Schatz, D. G.; Coleman, J. E.; Steitz, T. A. Crystal structure of the RAG1 dimerization domain reveals multiple zinc-binding motifs including a novel zinc binuclear cluster. *Nat. Struct. Biol.* **1997**, *4*, 586–591.
- (14) Nuber, U.; Schwarz, S.; Kaiser, P.; Schneider, R.; Scheffner, M. Cloning of human ubiquitin-conjugating enzymes UbcH6 and UbcH7 (E2–F1) and characterization of their interaction with E6-AP and RSP5. *J. Biol. Chem.* **1996**, *271*, 2795–2800.
- (15) Dawid, I. B.; Breen, J. J.; Toyama, R. LIM domains: multiple roles as adapters and functional modifiers in protein interactions. *Trends Genet.* **1998**, *14*, 156–162.
- (16) Matthews, J. M.; Kowalski, K.; Liew, C. K.; Sharpe, B. K.; Fox, A. H.; Crossley, M.; MacKay, J. P. A class of zinc fingers involved in protein-protein interactions: biophysical characterization of CCHC fingers from fog and U-shaped. *Eur. J. Biochem.* **2000**, *267*, 1030–1038.
- (17) Liu, H.-L.; Ho, Y.; Hsu, C.-M. The influence of metal ions on the substrate binding pocket of the human alcohol dehydrogenase $\beta_2\beta_2$ by molecular modeling. *Chem. Phys. Lett.* **2003**, *372*, 249–254.
- (18) Hwang, M.-J.; Ni, X.; Waldman, M.; Ewig, C. S.; Hagler, A. T. Derivation of class II force fields. VI. carbohydrate compounds and anomeric effects. *Biopolymers* **1998**, *45*, 435–468.
- (19) Kabsch, W.; Sander, C. Dictionary of protein secondary structure: pattern recognition of hydrogen-bonded and geometrical features. *Biopolymers* **1983**, *22*, 2577–2637.
- (20) Roehm, P. C.; Berg, J. M. Sequential metal binding by the RING finger domain of BRCA1. *Biochemistry* **1997**, *36*, 10240–10245.
- (21) Kentsis, A.; Borden, K. L. B. Construction of macromolecular assemblages in eukaryotic processes and their role in human disease linking RINGs together. *Curr. Protein Pept. Sci.* **2000**, *1*, 49–73.
- (22) Houben, K.; Wasielewski, E.; Dominguez, C.; Kellenberger, E.; Atkinson, R. A.; Marc Timmers, H. T.; Kieffer, B.; Boelens, R. Dynamics and metal exchange properties of C4C4 RING domains from CNOT4 and the p44 subunit of TFIIH. *J. Mol. Biol.* **2005**, *349*, 621–637.
- (23) Lai, Z.; Freedman, D. A.; Levine, A. J.; McLendon, G. L. Metal and RNA binding properties of the hdm2 RING finger domain. *Biochemistry* **1998**, *37*, 17005–17015.
- (24) Hanzawa, H.; de Ruwe, M. J.; Albert, T. K.; van der Vliet, P. C.; Marc Timmers, H. T.; Boelens, R. The structure of the C4C4 ring finger of human NOT4 reveals features distinct from those of C3HC4 RING fingers. *J. Biol. Chem.* **2001**, *276*, 10185–10190.

Received May 22, 2007. Accepted July 6, 2007.

BP0701665